Intelligent Robust-Switching PID Controller Design for a Micro-Actuator

Marialena Vagia, George Nikolakopoulos and Anthony Tzes
University of Patras
26500 Rio Achaia ,Greece
{mvagia,gnikolak,tzes}@ee.upatras.gr

***Abstract*— In this article the design of an intelligent robust controller for a Micro–Actuator ($\mu - A$) is presented. The $\mu - A$ is composed of a micro–capacitor, whose one plate is clamped while its other flexible plate's motion is constrained by hinges acting as a combination of springs and dashpots. The distance of the plates is varied by the applied voltage between them. The dynamics of the plate's rigid-body motion results in an unstable, nonlinear system. The control scheme is applied to multiple linear time invariant models of the $\mu - A$ from the linearization process in multiple points. This control scheme is constructed from: a) a feedforward controller which stabilizes the micro–actuator around its nominal operating point, b) a robust-switching PID controller which gains are firstly tuned via the utilization of Linear Matrix Inequalities (LMIs) and secondly they are switched during the simulation depending on the displacement of the upper plate, and c) an intelligent prefilter which shapes appropriately the reference signal. The resulting overall control scheme is applied to the non–linear model of the $\mu - A$ where simulation results are presented to prove the efficacy of the suggested scheme.**

***Index Terms*— Micro-actuator Modelling, Switching Control, LMI, PID-Tuning, Intelligent Filter Design**

I. INTRODUCTION

Micro–devices in the form of actuators and sensors are becoming increasingly dominant nowadays [1, 2] with the technological improvements in the area of micro–fabrications [3] setting new limits in the design of micro–devices. In the area of micro–actuators, several micro–structures [4, 5] have been used as the primitive components. These actuators could be utilized in many applications where the application of a force (picoNewtons), in conjunction with their positioning, is needed [6–8].

The utilization of modern μ–A demands new approaches regarding the control of these structures. Due to their diminution, there is a need to utilize advance control techniques for satisfying certain performance and control objectives [9]. These techniques primary stem from the modelling peculiarities of these devices as many factors that are ignored in the macro–world play an important role in the micro–world. Moreover the non-linearity of the μ–A model is forcing the control designer to linearize the model before applying the advance control techniques instead of relying on the design of non–linear controllers, which are very complicated to be implemented.

For the resulting multiple linearized models of the μ–actuator a combination of advanced control techniques and appropriate pre–filtering seems to be essential for a robust and high–quality control of this demanding μ–actuators.

In this article an LMI-based robust–switching PID controller is designed, whose gains are switched with respect to the state vector of the multiple linearized models of the nonlinear system. These transitions are active when there is a switch of the system from one linear model to another. This control design approach is based on: a) a feedforward controller that aims to stabilize the capacitor's plate around the selected nominal point of operation, b) a tuning process for the utilized LMIs for computing the PID–control action, and c) an intelligent–tuned pre–filtering process for shaping appropriately the reference signal prior to the controller excitation.

In the rest of this article the extraction of the $\mu - A$ model is carried in Section II, while the design of the controller is presented in Section III. In Section IV extended simulation studies that prove the efficacy of the proposed control scheme are presented. Finally in Section V the conclusions are drawn.

II. MICRO–ACTUATOR MODELLING

The μ-A from a dynamics point of view corresponds to a micro-capacitor whose one plate is attached to the ground while its other moving plate is floating in air. The boundary of the moving plate is either supported (pinned) or constrained by hinges (springs), as shown in Figure 1.

A. Dynamic Plate Model

The equation of motion for a 2-D distributed thin plate [10] floating on air and supported at its boundary is expressed as follows

$$\mathcal{L}w(x,y,t) + \mathcal{C}\dot{w}(x,y,t) + m_p\ddot{w}(x,y,t) = f(x,y,t), \quad (1)$$

where $\mathcal{L}$ is a time-invariant, symmetric, non-negative differential operator, $\mathcal{C}$ is a damping operator, m_p is the mass density of the 2-D structure, $f(x,y,t)$ is the time-varying distributed control force acting on the thin plate at the (x,y)–coordinate, and the structural proportional damping is $C = \alpha_1 + \alpha_2 m_p$.

This work was partially funded by the European Social Fund (ESF), Operational Program for Educational and Vocational Training II (EPEAEK II) and particularly the Program HERAKLEITOS, No. B238.012.

In thin plate theory the operator $\mathcal{L}w(x,y,t)$ is

$$\frac{Eh^3}{12(1-\nu^2)}\left(w_{xxxx}+2w_{xxyy}+w_{yyyy}\right), \tag{2}$$

where E is the Young's modulus, ν is the Poisson's ration of the plate material, h is the thickness of the plate, and the symbol w_{xy} corresponds to $\frac{\partial}{\partial x}\frac{\partial}{\partial y}w(x,y,t)$.

For a thin square plate of length ℓ, shown in Figure 1, the equations of motion along with its boundary conditions are:

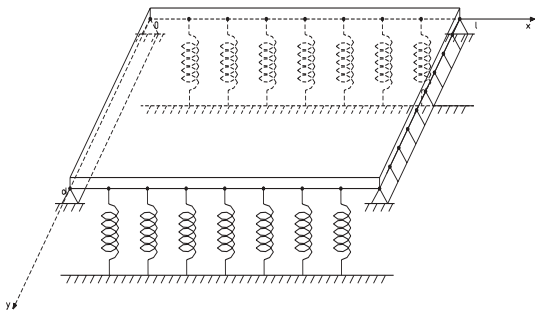

Fig. 1. μ-Actuator Thin Supporting Plate

$$\begin{aligned}
&w_{tt}+D_1(w_{xxxx}+2w_{xxyy}+w_{yyyy})=0,\\
&\qquad\qquad 0<x,y<\ell, t>0\\
&w(x,y,0)=w_0(x,y),\quad w_t(x,y,0)=w_1(x,y),\\
&\qquad\qquad 0<x,y<\ell,\\
&w(0,y,t)=w(\ell,y,t)=w_{xx}(0,y,t)=w_{xx}(\ell,y,t)=0,\\
&\qquad\qquad 0<y<\ell\\
&D(w_{yyy}+(2-\nu)w_{xxy})=-k^2w,\ y=0, 0<x<\ell\\
&D(w_{yyy}+(2-\nu)w_{xxy})=k^2w,\ y=\ell, 0<x<\ell\\
&w_{yy}+\nu w_{xx}=0,\ y=0, y=\ell, 0<x<\ell
\end{aligned}$$

where $D_1=\frac{D}{\rho}=\frac{Eh^3}{12m_p(1-\nu^2)}$, $w_0(x,y)$ $(w_1(x,y))$ is the initial displacement (velocity) of the plate in z-direction, and k represents the linear restoring force of the springs.

Application of the assumed modes method dictates that the displacement and point control force can be expressed as

$$w(x,y,t)=\sum_{i=1}^{\infty}W_i(x,y)\eta_i(t) \tag{3}$$

$$f(x,y,t)=\sum_{i=1}^{p}F_i(t)\delta(x-x_i)\delta(y-y_i) \tag{4}$$

where $\eta_i(t)$ is the ith mode modal displacement, $F_i(t)$ is the force amplitude, p is the number of actuators, $\delta(x-x_i)$ and $\delta(y-y_i)$ are spatial Dirac delta functions.

For the given stated boundary conditions, closed form solutions can be found [11] for the free-response expressions $w(x,y,t)$. Retaining a finite number of modes the ordinary differential equation describing the motion for the nth mode is

$$\ddot{\eta}_n+\left(\alpha_1\omega_n^2+\alpha_2\right)\dot{\eta}_n+\omega_n^2\eta_n=\sum_{i=1}^{p}W_n^*(x_i,y_i)F_i. \tag{5}$$

When: 1) the forcing element $f(x,y,t)=f(t)$ is independent of the point of application, 2) there is no proportional damping ($\alpha_1=0$), and 3) retaining only one mode ($n=1$) the equation of motion degenerates to

$$\ddot{\eta}_1+\alpha_2\dot{\eta}_1+\omega_1^2\eta_1=W_1^*F. \tag{6}$$

The resulting movement that this mode produces is displayed in Figure 2. In this case, the displacement of the plate $z(t)=w(x,y,t)$ is identical for all points (x,y) of the plate and equal to $\eta_1(t)$. Multiplication of both sides of (6) by $W_1^*=m$ yields the following equation of motion $m\ddot{\eta}_1+b\dot{\eta}_1+k\eta_1=F$, where m is the total mass of the plate, and k is the overall stiffness of the springs, as shown in Figure 3.

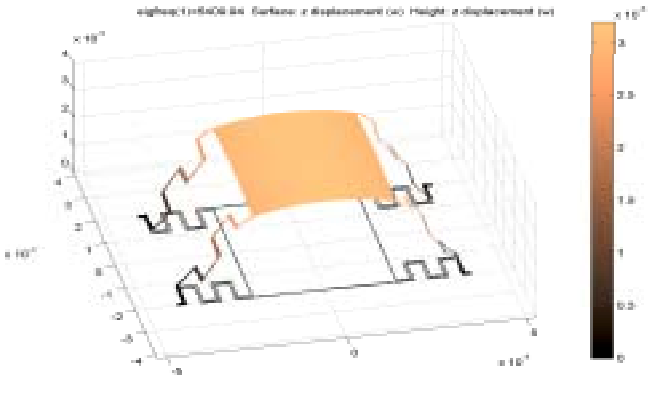

Fig. 2. μ-Actuator's 1st–Vibrational mode

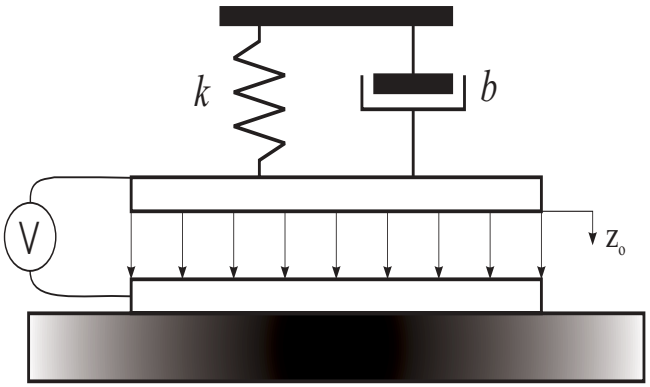

Fig. 3. Rigid body dynamical modelling

B. Electrical Force Model

Application of a voltage U between the capacitor's plates generates an electrically–induced force

$$F_x=\frac{\varepsilon AU^2}{2s^2},$$

where A is the area of the plates, ε is the dielectricic constant and s is the distance between the plates when the spring is relaxed.

The nonlinear equation of motion for the displacement x from the equilibrium point is given by [12]

$$m\ddot{\eta}_1+b\dot{\eta}_1+k\eta_1=\frac{aU^2}{(s-\eta_1)^2} \tag{7}$$

and $a = \frac{\varepsilon A}{2}$.

The "equilibria"-points $\eta^o_{1,i},\ i = 1, \ldots, M$ depend on the applied nominal voltages U_o. Equation (7) for $\dot{\eta}^o_{1,i} = 0$ yields

$$k\eta^o_{1,i} = \frac{aU_o^2}{(s-\eta^o_{1,i})^2} \quad U_o = \pm\left[\frac{k\eta^o_{1,i}\left(s-\eta^o_{1,i}\right)^2}{a}\right]^{1/2} . \quad (8)$$

This nominal U_o–voltage must be applied if the capacitor's plate is to be maintained at a distance $\eta^o_{1,i}$ from its un–stretched position.

The linearized equations of motion around the equilibria points $\left(U_o, \eta^o_{1,i}, \dot{\eta}^o_{1,i} = 0\right)$ can be found using standard perturbation theory for the variables U and η_1 where $U = U_o + \delta u$ and $\eta_{1,i} = \eta^o_{1,i} + \delta\eta_{1,i}$. The equation of motion for the perturbed system is:

$$\begin{aligned} m\delta\ddot{\eta}_{1,i} + b\delta\dot{\eta}_{1,i} + k\eta^o_{1,i} + k\delta\eta_{1,i} &= \frac{aU_o^2}{(s-\eta^o_{1,i})^2} \\ &+ \frac{2aU_o^2}{(s-\eta^o_{1,i})^3}\delta\eta_1 + \frac{2aU_o}{(s-\eta^o_{1,i})^2}\delta u \quad (9) \end{aligned}$$

Inserting the expression from (8) into (9) we obtain

$$m\delta\ddot{\eta}_{1,i} + b\delta\dot{\eta}_{1,i} + K_i\delta\eta_1 = \beta_i\delta u\ , \quad (10)$$

where $K_i = \left[k - \frac{2aU_o^2}{(s-\eta^o_{1,i})^3}\right]$, and $\beta_i = \left[\frac{2aU_o}{(s-\eta^o_{1,i})^2}\right]$. The state space description of (10) is

$$\begin{aligned} \begin{bmatrix} \delta\dot{\eta}_{1,i} \\ \delta\ddot{\eta}_{1,i} \end{bmatrix} &= \begin{bmatrix} 0 & 1 \\ -\frac{K_i}{m} & -\frac{b}{m} \end{bmatrix}\begin{bmatrix} \delta\eta_{1,i} \\ \delta\dot{\eta}_{1,i} \end{bmatrix} + \begin{bmatrix} 0 \\ \frac{\beta_i}{m} \end{bmatrix}\delta u \quad (11) \\ &= \tilde{A}_i\begin{bmatrix} \delta\eta_{1,i} \\ \delta\dot{\eta}_{1,i} \end{bmatrix} + B_i\delta u, \quad i = 1, \ldots, M. \quad (12) \end{aligned}$$

III. Intelligent Switching– Controller Design

Mathematically, a switched linear control system can be described by:

$$\begin{aligned} x(k+1) &= A_i x(k) + B_i u(k) \quad (13) \\ y(k) &= C_i x(k) \end{aligned}$$

where $x \in R^n$ is the state, $u \in R^p$ is the input, $y \in R^q$ is the output, and i is a piecewise constant switching signal that takes values from the finite index set $F = 1, 2, \ldots, M$ [13]. Given the structure of each individual subsystem, the overall system behavior is determined by the switching signal. In general a switching signal i may depend on its past value, the time, and the state/output. The last case is the one that is active in our modelling approach of the μ–A.

Based on the switching modelling in (13) of the μ–A, a robust PID controller [14] is designed for every switched subsystem. The resulting switching robust PID controller is combined with a Feedforward Controller (FC) and an Intelligent Prefilter as shown in Figure 4. The lowpass prefilter acts on the reference signal; its cut–off frequency is tuned according to the spectrum of the reference signal. The FC-term provides the U_o portion in (8).

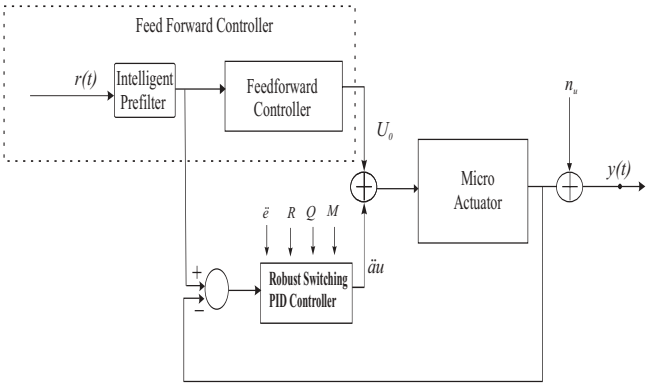

Fig. 4. LMI–based Robust–Switching PID Control Architecture

A. Robust-Switching PID–Controller Design

The feedback term is a robust–switching PID controller for the set of the M–linearized systems in (12).

The LMI–based [15], switching [16], PID controller design procedure is based on the theory of Linear Quadratic Regulator (LQR) and on the theory of Switched linear Control Systems.

This robust–switching PID controller is specially designed to address to the case where multiple–models [17–19] have been utilized in order to describe the uncertainties that are inherent from the linearization process of the non–linear system model.

The nature of a PID–structure in the controller design can be achieved if the the linearized system's state vector $\bar{\eta} = \left[\delta\eta_{1,i}, \delta\dot{\eta}_{1,i}\right]^T$ is augmented with the integral of the error signal $\int edt = \int\left(r(t) - \eta_{1,i}(t)\right)dt$. In this case, the augmented system's description is

$$\begin{bmatrix} \dot{\bar{\eta}} \\ -e \end{bmatrix} = \hat{A}_i\begin{bmatrix} \bar{\eta} \\ -\int edt \end{bmatrix} + \begin{bmatrix} B_i \\ 0 \end{bmatrix}\delta u + \begin{bmatrix} -1 \\ 0 \end{bmatrix} r, \quad (14)$$

where $\hat{A}_i = \begin{bmatrix} \tilde{A}_i & 0 \\ 1 & 0 \end{bmatrix}$.

The LQR–problem for the systems described in (14) can be cast in the computation of δu in order to minimize the cost:

$$J(\delta u) = \int_0^\infty (\tilde{\eta}^T\ Q\ \tilde{\eta} + \delta u^T\ R\ \delta u)dt \quad (15)$$

where $\tilde{\eta} = \left[\bar{\eta}, -\int edt\right]^T$, and Q, R are semidefinite and definite matrices respectively. Rather than using the $\hat{A}_i$–matrices in the LQR–problem, the introduction of the auxiliaries matrices $A_i = \hat{A}_i + \Lambda\mathbf{I}$, where $\Lambda > 0$ and $\mathbf{I}$ the identity matrix generates an optimal control $\delta u = -S\bar{\eta}$ such that the closed–loop's poles have real part less than $-\Lambda$, or $\Re(\text{eig}(\hat{A}_i - BS)) < -\Lambda\ \forall i \in \{1, \ldots, M\}$.

The optimal control $\delta u = -S\tilde{\eta}$ can be computed via the following LMI–based algorithm, where a set of auxiliary matrices $\hat{P},\ Y$ and an additional variable γ $(\gamma > 0)$ have been introduced.

1) Start with a large value of γ.

2) Compute a feasible solution $\hat{P}, Y$ (if exists) to the following set of convex constraints:

$$\left[\begin{array}{cc} \gamma & \tilde{\eta}^T(0) \\ \tilde{\eta}(0) & \hat{P} \end{array} \right] \leq 0 \quad (16)$$

For $i = 1, \ldots, M$

$$\left[\begin{array}{ccc} A_i\hat{P} + \hat{P}A_i^T + B_iY + Y^TB_i^T & \hat{P} & Y^T \\ \hat{P} & -Q^{-1} & 0 \\ Y & 0 & -R^{-1} \end{array} \right] \leq 0 \quad (17)$$

$$\hat{P} > 0 \quad (18)$$

3) Reduce γ by $\delta\gamma$ ($\gamma - \delta\gamma \rightarrow \gamma$) and Return to Step 1.

The feedback control can be computed based on the recorded values of $\hat{P}^*$ and Y^* for the last feasible solution:

$$\delta u = Y^*(\hat{P}^*)^{-1}\tilde{\eta} = -S\tilde{\eta} = -S \left[\begin{array}{c} \bar{\eta} \\ -\int edt \end{array} \right] \quad (19)$$

$$= - \left[\begin{array}{c|c|c} s_p & s_d & s_i \end{array} \right] \left[\begin{array}{c} \delta\eta_{1,i} \\ \delta\dot{\eta}_{1,i} \\ -\int edt \end{array} \right]$$

$$= \left[s_p e + s_d \dot{e} + s_i \int edt \right] + \left[s_p \left(\eta_{1,i}^o - r \right) - s_d \dot{r} \right] \quad (20)$$

The first portion of the controller form in (20) is equivalent to that of a PID–controller.

The applied controller although, is a switching one which values are being switched during the simulation, with the switching rule to be the first state of the system, which indicates the distance between the upper plate of the capacitor and the final position, and forces the non–linear system to switch among distinct linear time invariant state space models.

B. Intelligent Prefilter Design

The scope of the Intelligent Preshaping Filter (IPF) is to suppress the high harmonics of the excitation signal, particularly in the case of high speed maneuvers. This is due to the nonlinear (quadratic) nature of the system in (7), where second harmonic resonances can be developed. These second harmonic resonances can de generated either from the output of the PID-controller, or from the feedforward term. Indirectly, the output from both of these portions is influenced from the spectrum content of the reference signal $r(t)$.

A simple first order lowpass filter of the form $G_{IF} = \frac{p}{s+p}$ is used for appropriately shaping the reference signal,as shown in Figure 5. The selection of the cutoff frequency "p" is made in order to: a) extend the robustness of the system towards large variations of the spectrum content of the reference signal, and b) decrease the response time of the system in small maneuvers. These two objectives are in conflict since for the first case a reduction of the filter bandwidth of the system is needed while for the second case an increase of the filter bandwidth is necessary for decreasing the system's response time. In this research effort, the p–parameter is tuned based on an intelligent ad–hoc procedure.

The spectrum content of the reference signal can be captured through the usage of the Fourier transform. Under

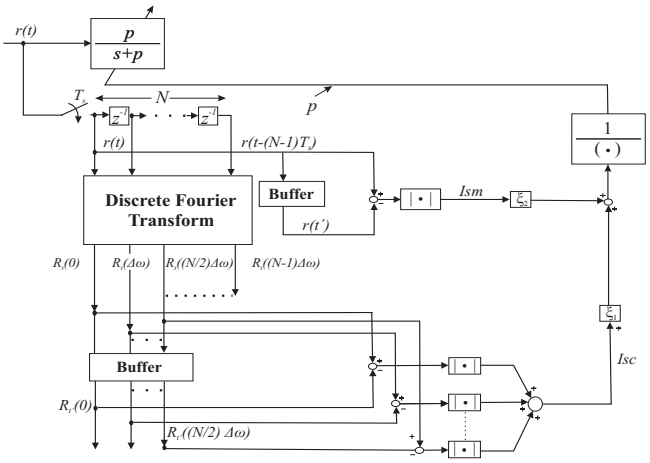

Fig. 5. Tuning Scheme of Intelligent Prefilter

the assumption that the reference signal $r(t)$ is sampled with a period of T_s, its harmonic content over the last N–samples $(r(t-(N-1)T_s), \ldots, r(t-T_s), r(t))$ can be computed via the Discrete Fourier Transform. Let the frequency transformed signal over the sliding window NT_s at time t be $\mathcal{R}_t(\omega)$, $\omega \in \Delta\omega\{0, \ldots, (N-1)\}$, where $\Delta\omega = \frac{2\pi}{NT_s}$; an index describing variations of spectrum content between different time instants $t^{'}$ and t can be of the form

$$I_{sc} = \sum_{j=0}^{\frac{N}{2}} \left| \mathcal{R}_{t'}(j\Delta\omega) - \mathcal{R}_t(j\Delta\omega) \right| \ . \quad (21)$$

Large values of I_{sc} indicate a dissimilarity between $\mathcal{R}_{t'}(\omega)$ and $\mathcal{R}_t(\omega)$.

Similarly the notion of a "small maneuver" can be captured by the difference

$$I_{sm} = \left| r(t^{'}) - r(t) \right| \ . \quad (22)$$

¿From the aforementioned discussion, the p-cutoff frequency should be inverse proportional to the I_{sc} and I_{sm}, or

$$p = \frac{1}{\xi_1 I_{sc} + \xi_2 I_{sm}} \ , \quad (23)$$

where $\xi_1, \xi_2 \geq 0$.

IV. Simulation Studies

Simulation studies were carried on a $\mu - A$'s non-linear model, whose its SiO_2–plates have an area $A = 400\mu$m $\times 400\mu$m, with a mass $m = 7.0496 \cdot 10^{-10}$ Kgr. The initial gap was set to $s = 4\mu$ m while the dielectric constant of the air was $\varepsilon = 9 \cdot 10^{-12} \frac{\text{Coulomb}^2}{N \cdot m^2}$. The allowable displacements of the micro–capacitor's plate in the vertical axis were $\eta_1 \in [0.1, 3.9]\,\mu$ m. The goal of the controller was to move the capacitor's plates from an initial position to a new desired one (set–point regulation). Two distinct cases, as far as the number of "switching" points were examined: 1)Single switching point for the values of the controller and $\eta_{1,1}^o = 1.9\mu$m, and 2) Ten switching points

and $\eta^o_{1,i} = 0.1 + \frac{3.9-0.1}{2\cdot 10} + (i-1)0.38\mu$m, $i = 1, \ldots, 10$. Each set of the parameters of the controller is switching every time that there is a movement of the upper plate from its initial to its final position and their distance is higher than 0.38μ m.Also, it is valid only in the calculated region(i.e., for the movement of the plate from 0.1μm to 2.5μm the set of the parameters will change 6 times in the next points: $(0.48, 0.86, 1.24, 1.62, 2, 2.3)\mu m$).

The proposed control scheme has been applied in multiple simulation test cases in order to test its efficacy. Particular attention has been paid in order to identify any relevance among the number of the switching points and the performance of the controller on the nonlinear system. In the sequel, unless otherwise stated the parameters used in the formulation of the LQR–cost were $R = 10^{-5}$ and $Q = 10^{-3}\mathbf{I}_{3\times 3}$. Similarly, the measurements are assumed to be corrupted noise of level such that the SNR=20db. The cutoff of the filter p floats in the range between 200 and 2000 $\frac{\text{rad}}{\text{sec}}$; the parameters used for its adjustment were $\xi_1 = 0.05$, $\xi_2 = 0.95$, $T_s = 10$ nsec, and $N = 128$ samples. Since the I_{sm} dominates the adjustment of the filter's cutoff, Figure 6 presents in a graphical manner the relationship between p and I_{sm}.

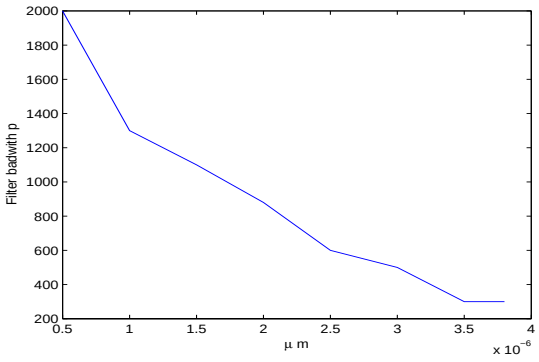

Fig. 6. Dependence between p–parameter and displacement I_{sm}

The micro-actuator while at rest at 0.1μm ($\eta_1(0) = 0.1\mu$m) is excited with a step signal of amplitude 2.5×10^{-6} at time 0.01 seconds. In Figure 7 we present the responses of the micro–capacitor for one switching point and two cases of "prescribed" stability , namely i) $\Lambda = 1$, and ii) $\Lambda = 90$. As expected, the system responds faster in the second case since it is guaranteed that its closed-loop poles will have real part less than -90 (and that is for all the sets of the switching parameters of the PID). For the case that there is only one switching point at the values of the controller during the simulation the step responses of the micro–capacitor and the relevant control effort are displayed in Figures 7, 8, 9 respectively.

For the case of 10–switching points for the gains of the controller the step responses of the micro–capacitor and the relevant control effort are displayed in Figures 10, 11, 12 respectively.

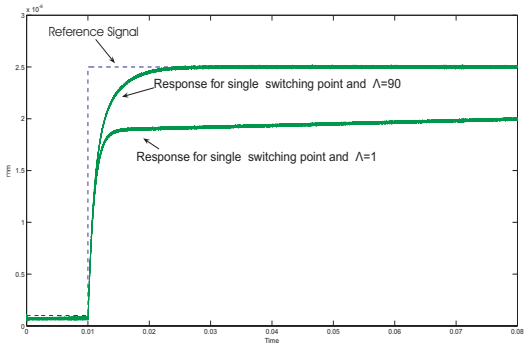

Fig. 7. Micro-actuator step response (Single switching point, $\Lambda = 1$ and $\Lambda = 90$)

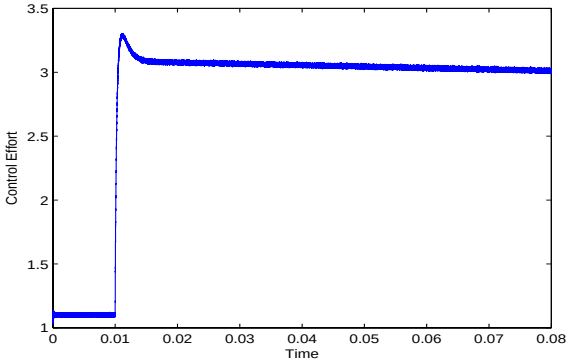

Fig. 8. Controller effort (Single Switching point, $\Lambda = 1$)

V. Conclusions

In this article an intelligent controller has been designed for a micro–actuator system. The controller consists of: a) a feedforward portion, b) a switching PID-controller, and c) an intelligent prefilter. The switching parameters of the feedback controller are tuned via the usage of LMIs while the cutoff of the IPF is tuned in an ad–hoc manner suited for the nonlinear nature of the $\mu - A$. The efficiency of the suggested scheme, as well its sensitivity on certain parameters is tested in a series of simulation studies. The controlled system has a superior performance (tracking behavior) in the case of the utilization of the switching controller, compared with the case of the single LMI–based PID controller.

Although the produced, LMI–based PID controllers, guarantee that the sontrol system will remain stable in every operating region that the controller has been calculated, the insertion of the switchings among the controllers does not provide any guarantee regarding stability. Extended theoretically studies will be carried in the future work towards the stability investigations of the suggested scheme.

References

[1] E. Lyshevski, "Microelectromechanical systems: Motion control of microactuators.," in *IEEE/ASME Transactions on Mechatronics Proceedings of the IEEE Conference on Decision and Control*, 1998.

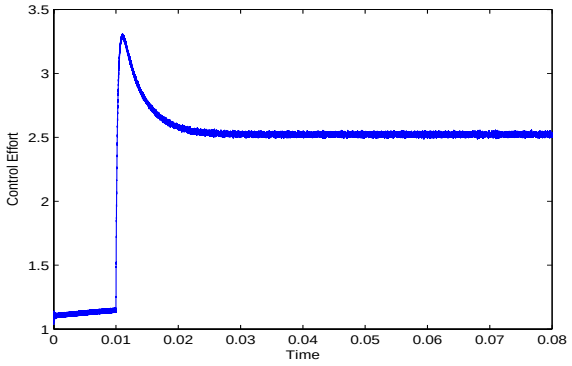

Fig. 9. Controller effort (Single Switching point, $\Lambda = 90$)

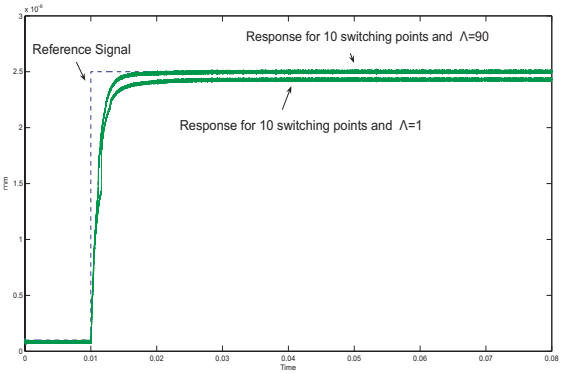

Fig. 10. Micro-actuator step response (10 switching points, $\Lambda = 1$ and $\Lambda = 90$)

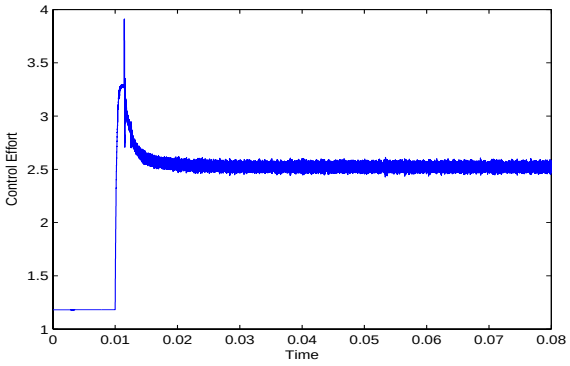

Fig. 11. Controller effort (10 Switching points, $\Lambda = 1$)

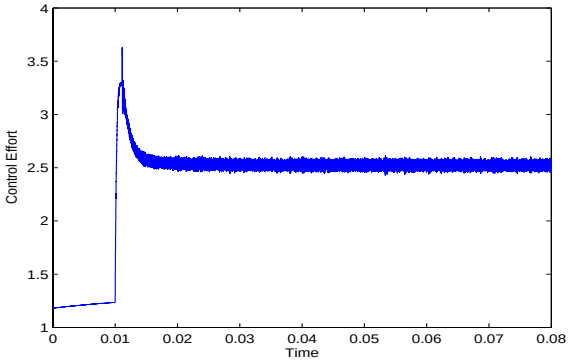

Fig. 12. Controller effort (10 Switching points, $\Lambda = 90$)

[2] A. Menciassi and A. Eisinberg and I. Izzo and P. Dario, "From "macro" to "micro" Manipulation: Models and Experiments," in *IEEE-ASME Transactions on Mechatronics*, vol. 9, pp. 311–320, 2004.

[3] M. Madou, *Fundamentals of Microfabrication*. CRC PRESS, Boca Raton, FL, 1997.

[4] M. Sitti, "Survey of Nanomanipulation Systems," *IEEE-Nanotechnology Conference*, pp. 75–80, November 2001.

[5] H. Ishihara, F. Arai, and T. Fukuda, "Micro mechatronics and micro actuators," *IEEE/ASME Transactions on Mechatronics*, vol. 1, pp. 68–79, March 1996.

[6] A. Lee, C. McConaghy, G. Sommargren, P. Krulevitch, and E. Campbell, "Vertical - actuated electrostatic comb drive with in situ capacitive position correction for application in phase shifting diffraction interferometry," *Journal of Microelectromechanical Systems*, vol. 12, pp. 960–971, December 2003.

[7] H. Liu, B.Lu, Y. Ding, Y. Tang, and D. Li, "A motor - piezo actuator for nano - scale positioning based on dual servo loop and nonlinearity compensation," *Journal of Micromechanics and Microengineering*, vol. 13, pp. 295–299, March 2003.

[8] H. Zhang, A. Laws, V. Bright, K. Gupta, and Y. Lee, "MEMS variable - capacitor phase shifters Part I: Loaded - line phase shifter," *International Journal of RF and Microwave Computer - Aided Engineering*, vol. 13, pp. 321–337, July 2003.

[9] E. Lyshevski, "Micro–electromechanical systems: Motion control of micro–actuators," *Proceedings of the IEEE Conference on Decision and Control*, 1998.

[10] S. Hong, V. Varadan, and V. Varadan, "Implementation of coupled mode optimal structural vibration control using approximated eigenfunctions," *Smart Material Structures*, vol. 7, pp. 63–71, 1998.

[11] M. Zarubinskaya and W. Horssen, "On the free vibrations of a rectangular plate with two opposite sides simply supported and the other sides attached to linear springs," report 03–09, DELFT University of Technology, 2003.

[12] A. Tzes, G. Nikolakopoulos, L. Dritsas, and Y. Koveos, "Multi–parametric H_∞ control of a μ–actuator," *In the Proceedings of the 2005 IFAC World Congress*, (Prague, Czech), July 2005 (to appear).

[13] Z. Sun and S. Ge, "Analysis and Synthesis of Swithced Linear Control Systems," *Automatica.*, vol. 41, pp. 181–195, 2005.

[14] M. Ge, M. Chiu, and Q. Wang, "Robust PID controller Design via LMI approach," *Journal of Process Control*, vol. 12, pp. 3–13, 2002.

[15] J. VanAntwep and R. Braatz, "A tutorial on linear and bilinear Matrix Inequalities ," *Journal of Process Control*, vol. 10, pp. 363–385, 2000.

[16] S. Zhendong and S.S. Ge, "Analysis and Synthesis of Switched linear Control Systems," *Automatica*, vol. 41, pp. 181-195, 2005.

[17] K. Narendra, J. Balakrishnan, and M.K.Ciliz, "Adaptation and Learning using multiple models ,switching and tuning," *IEEE Control Systems Magazine*, vol. 15, pp. 37–51, 1995.

[18] Y. Cheng and C. Yu, "Nonlinear process control using multiple models:relay feedback approach ," *Industrial Eng.Chem.*, vol. 39, pp. 420–431, 2000.

[19] C. Chen, "A simple method for on-line identification and controller tuning," *AIChE*, vol. 35, pp. 2037–2039, 1989.